ORGANOMETALLICS

Article

pubs.acs.org/Organometallics

Benzothiaoline Three-Coordinated Organoboron Compounds with a B═N Bond: Dual Emission and Temperature-Dependent Excimer Fluorescence

Soren K. Mellerup and Suning Wang*

Department of Chemistry, Queen's University, Kingston, Ontario K7M 3N6, Canada

Supporting Information

ABSTRACT: A series of 2,2-disubstituted benzothiazoline-$BMes_2$ (Mes = mesityl) compounds containing a B═N bond have been prepared and fully characterized. Their photophysical properties were investigated by UV−vis and fluorescence spectroscopy, which revealed the presence of solvent- and concentration-dependent dual emission. On the basis of the spectroscopic data, the dual emission was assigned to monomer and excimer fluorescence of the molecule, respectively. Experimental and TD-DFT computational data indicated that the purple-blue monomer emission of these compounds is mainly from an intramolecular charge transfer (CT) transition between the benzo-sulfur moiety and the boron center. The yellow-green excimer emission is attributed to intermolecular interactions involving the benzo-sulfur unit. Furthermore, the excimer emission maxima of all compounds were found to be sensitive to temperature, shifting to lower energy with decreasing temperature, which illustrates the potential for this class of compounds to be used as luminescent thermometers.

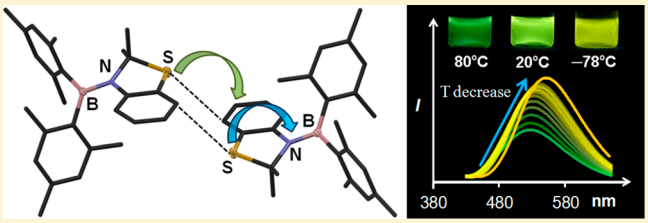

INTRODUCTION

The absorption of electromagnetic radiation by conjugated organic scaffolds has long been known to induce either photophysical or photochemical change. Of late, it has become well-established that the incorporation of a boron atom into such systems can lead to a drastic change in their elicited photoresponses.[1] In the case of three-coordinated boron compounds, the vacant p_π orbital of the boron atom typically improves the electron transport capability of the materials and consequently allows for fine-tuning of their photophysical properties.[2] Interestingly, the incorporation of four-coordinated boron centers can result in materials that behave significantly differently in response to photoexcitation. There are now several examples[3] of such species which undergo some form of photochemical transformation (i.e., isomerization or elimination) upon irradiation. Given the wide and tunable range of properties offered by organoboron materials, it should come as no surprise that much effort has gone into developing new boron-containing materials for use in applications such as organic light-emitting diodes[4] and memory devices.[5]

Recently, we reported the unusual multistructural transformation of N,C-chelated $BMes_2$ compounds bearing an azole unit (e.g., thiazole), wherein the azole unit was transformed to an azoline (**A** in Scheme 1) via an intramolecular H atom transfer.[3h] Subsequent photo- or thermal isomerization allowed for the controlled and reversible inversion of stereochemistry at the C2 position of the azoline moiety, which was believed to be made possible by the presence of the B═N bond in **A** and its diastereomer. In order to investigate whether light and heat could be used to control the chirality of azolines within simpler

Scheme 1. Previously Studied Organoboron Isomerization Process and Proposed Synthetic Targets 1−4

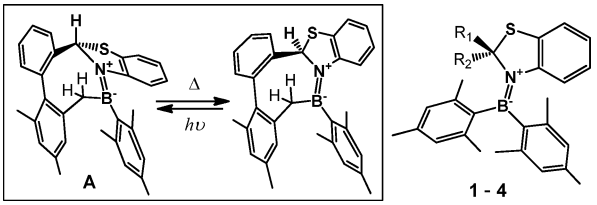

organonboron systems, we designed and synthesized benzothiazoline-$BMes_2$ compounds (**1−4**, Scheme 1 and 2) and examined their response to light and heat. Unfortunately, the thermal and photoisomerisation pathways that invert the azoline stereochemistry were found to be inaccessible in this new class of compounds. They do however display unusual dual intramolecular and intermolecular emission[6] in the purple-blue and yellow-green region respectively, which is sensitive to concentration, solvent polarity and temperature. Temperature-dependent fluorescent molecules have important applications in cellular imaging as molecular thermometers.[7] A few recent studies have shown that organoboron compounds are very promising as molecular thermometers due to their polarized excited states which are sensitive to temperature-dependent conformational change or proton transfer processes.[6e,8] Nonetheless, examples of temperature-dependent fluorescent orga-

Received: July 23, 2014

   dx.doi.org/10.1021/om500757r | *Organometallics* XXXX, XXX, XXX−XXX

noboron molecules over a wide temperature range remain rare and underexplored. For these reasons, we set out to investigate the curious fluorescent properties of the new class of B═N containing molecules and the results are reported herein.

RESULTS AND DISCUSSION

Syntheses and Structures. The benzothiazoline ligands and their $BMes_2$ compounds were readily synthesized under mild conditions as illustrated in Scheme 2. The 2,2-disubstituted benzothiazolines were all prepared in good yields by employing a solvent-free method described in the literature.[9] The B═N species **1**−**4** were subsequently obtained by first reacting the ligands with NaH to generate their sodium salts in situ, followed by a stoichiometric addition of $BMes_2F$ to afford **1**−**4** in ∼50% yield. The intense green-yellow fluorescence of **1**− **4** was qualitatively observed immediately following the addition of the boron source with a hand-held UV lamp (365 nm excitation). Compounds **1**− **4** were fully characterized by ^1H, ^{13}C, and ^{11}B NMR, HRMS, and elemental analysis. The ^{11}B NMR chemical shifts were found to be 47.8, 48.1, 48.3, and 48.3 ppm for **1**−**4**, respectively. These values reside in the typical range for three-coordinated organoboron[2] and are similar to those of previously reported three-coordinated boron compounds with a B═N bond.[3h,10]

Scheme 2. Synthetic Procedure for 1−4

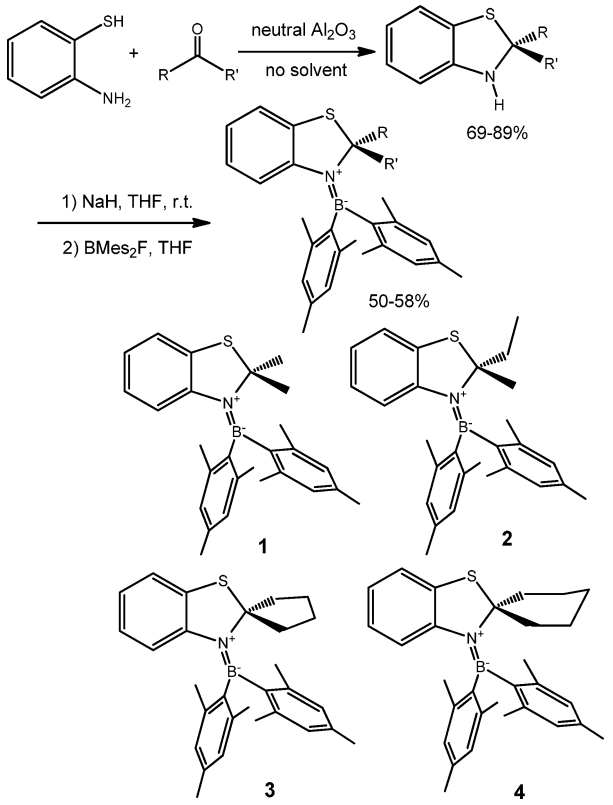

Compounds **1**−**4** were found to display dynamic exchange behavior in solution. In the ^1H NMR spectrum of compound **1** at room temperature (see Supporting Information (SI)), each mesityl group displays two distinct sets of chemical shifts indicating no free rotation about the B═N bond. This result is consistent with the previous finding that rotation around the B═N bond has a very large barrier.[11] At low temperature, the *o*-methyl pair on each mesityl is resolved, supporting the asymmetric structure of **1**, which undergoes a relatively fast chemical exchange at ambient temperature. Using the variable temperature data shown in Figure 1, the rotation barrier around the B−C bond was estimated[12] to be ca. 12 kcal mol^{-1}, which is in agreement with previously reported three-coordinated organoboron species.[2,10] The ^1H NMR spectrum of **2** shows well resolved chemical shifts for all of its methyl groups at 298 K as a result of the chiral C2 center. Upon cooling to 228 K, the ^1H NMR spectrum of **2** (see SI) shows two sets of well-resolved signals that can be assigned to the two diastereomers of **2** due to the asymmetric environment around the boron center and the C2 atom. The mesityl rotation around the B−C bond interconverts the diastereomers of **2** and this rotation barrier was estimated to be similar to that of **1**. Although the mesityl rotation barriers for compounds **3** and **4** were not directly measured, both of their ^1H NMR spectra are similar to that of compound **1**. Therefore, it is reasonable to suggest that they would also possess similar B−C rotation barriers. Compounds **1**−**4** decompose slowly in solution upon extended exposure to ambient conditions, generating the hydrolyzed product $(BMes_2)_2O$ or $BMes_2(OH)$ and the free ligand.[10] Interestingly, the same hydrolysis phenomenon was not observed for the related molecules **A** shown in Scheme 1.

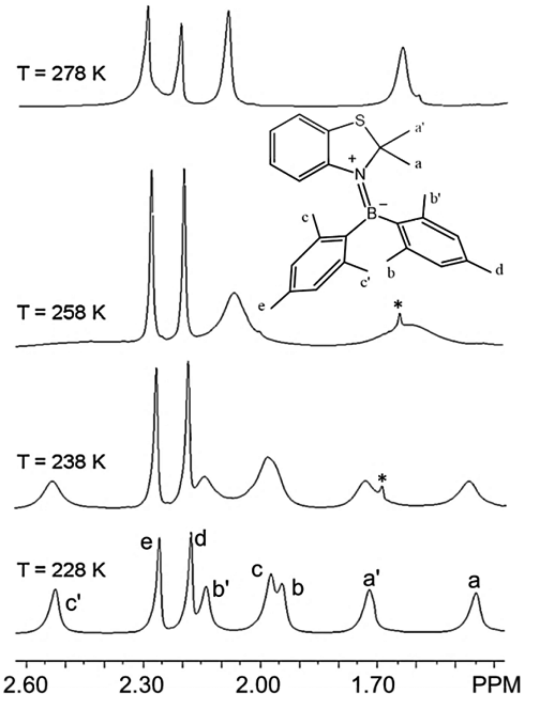

Figure 1. Variable temperature ^1H NMR spectra of **1** in CD_2Cl_2, where * represents an unidentified impurity.

The crystal structure of compound **1** was determined by single-crystal X-ray diffraction analysis and is shown in Figure 2. The boron center adopts a trigonal planar geometry with C(10)—B−C(19), C(10)—B−N, C(19)—B−N bond angles of 120.11(13)°, 120.24(15)°, 119.63(14)°, respectively, indicating minimal steric strain around the boron center. The five-membered thiazoline ring is puckered, causing the asymmetric environment for the two methyl groups at the 2-position. The crystal structure confirmed the presence of a B═N bond in **1**, as evidenced by the short B(1)−N(1) bond length, 1.428(2) Å, which is shorter than those observed in indolyl-$BMes_2$

dx.doi.org/10.1021/om500757r | *Organometallics* XXXX, XXX, XXX−XXX

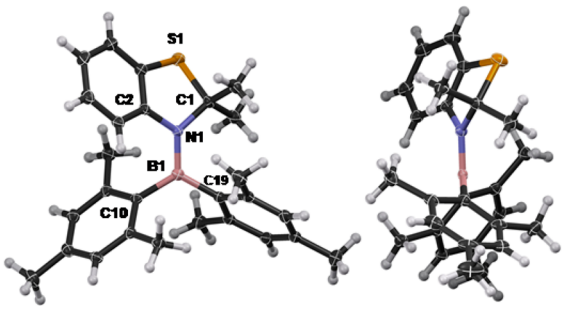

Figure 2. X-ray crystal structure of **1** with 35% thermal ellipsoids (top view and side view).

compounds that possess a B═N bond of ∼1.44 Å,[10] but comparable to other B═N bond lengths reported for R_2B═NR'_2 and azaborines.[3f,11,13] The two trigonal BNC_2 and NBC_2 planes are not coplanar but have a dihedral angle of 156.3°, as shown by the side view of the crystal structure in Figure 2. This is clearly caused by the steric interactions between the benzothiazoline ring and the mesityl rings. In the crystal lattice of **1**, no π-stacking interactions were observed.

There are however short intermolecular contacts between the S atom, the benzo ring and the mesityl ring, as shown in Figure 3. Due to the lack of suitable crystals, the structures of

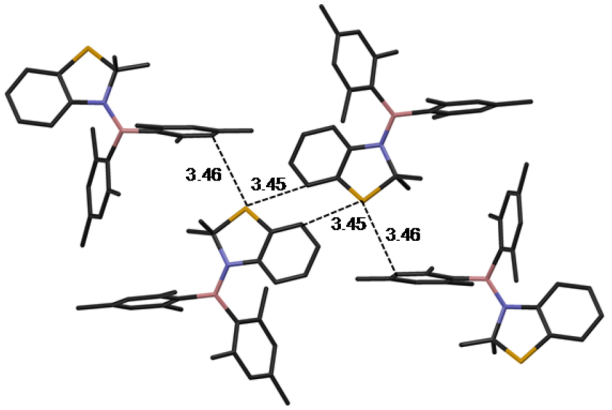

Figure 3. Short contacts observed in the crystal lattice of **1**.

2–**4** were not determined by X-ray diffraction analysis. For comparison, the structures of **1**–**4** were calculated and optimized by DFT calculations and are shown in Figure 4. For **1**, the calculated parameters match well with those from the crystal structure. In the structures of **3** and **4**, the cyclopentyl and the cyclohexyl rings adopt a puckered and a chair conformation, respectively, with the S atom occupying the axial position. The calculated B═N bond lengths in all four compounds are similar. Based on the torsion angles between BC_2 and NC'_2 units (φ of C → B→N → C′, see Table 1), compounds **2** and **4** are more congested than **1** and **3**.

Fluorescence of Compounds 1–4. As with many boron-containing organic frameworks, compounds **1**–**4** fluoresce in the UV–vis range of the electromagnetic spectrum. The UV–vis absorption spectra of these compounds are shown in Figure 5. In accordance with our previously reported indole-$BMes_2$ compounds,[10] all four boron compounds possess two major absorption bands in the UV region (ca. 298 and 320 nm) that do not change significantly with solvent polarity. In order to understand the origin of these absorption maxima, TD-DFT

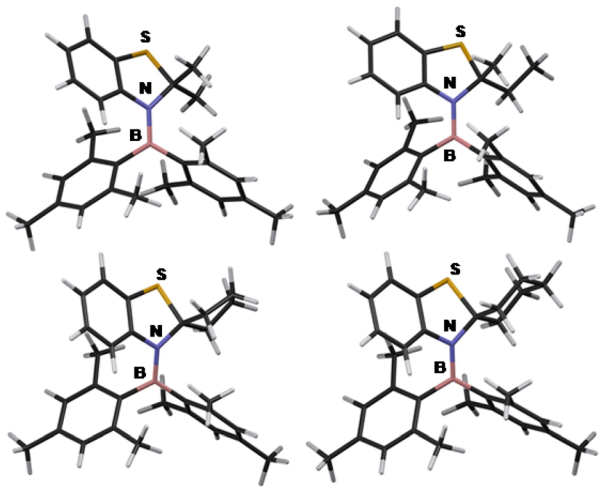

Figure 4. DFT optimized structures of **1**–**4**.

calculations for each compound using their computationally optimized geometries were performed. In all four cases, the predicted UV–vis spectra were found to be in good agreement with experimentally observed ones (see SI). The $S_0 \rightarrow S_1$ transition for all compounds involve mainly HOMO → LUMO (>90%) with a very large oscillator strength. For all four compounds, the HOMO is concentrated on the benzo ring and the sulfur atom with a small contribution from the B═N bond while the LUMO is dominated by the p_π orbital of the boron atom with significant contributions from the π^* orbitals of the benzo ring and the mesityl. Thus, the absorption band at ∼320 nm could be assigned to charge transfer from benzo-S to B (π^*). The sulfur atom has not only a large contribution to the HOMO level but also dominates the HOMO−1 level as shown in Figure 6. There appears to be minimal contributions to the electron density from the substituents at the 2-position on the benzothiazoline backbone which causes all the calculated HOMO and LUMO energy levels of **1**–**4** to look nearly identical. This result was expected, however, as the UV–vis spectra of the four compounds are also very similar. The high energy absorption bands at wavelengths <320 nm are mainly from the $\pi \rightarrow \pi^*$ transition of the benzothiazoline ring (**1** and **2**) or the mesityl (π) → B (π^*) transition (**3** and **4**) (see SI).

Compounds **1**–**4** emit a green or yellow color when irradiated at 365 nm with a hand-held UV lamp. This observation was rather unexpected because of the nonemissive and nonconjugated benzothiaoline backbone and the fact that the related indolyl-$BMes_2$ compounds in which the B atom is bound to a conjugated indole ring are blue fluorescent.[10] Upon further investigation, we observed that the luminescent color of **1**–**4** is strongly dependent on their concentration in solution. For example, at [**1**] = 10^{-6} M in THF an emission peak in the purple-blue region with λ_{max} = 374 nm was observed (Figure 7). As the concentration of **1** was increased from 10^{-6} to 10^{-2} M, the 374 nm emission peak was replaced by a broad green emission band centered at 529 nm with minimal change in the accompanying excitation spectra. Similarly, this same phenomenon was also observed for compounds **2**–**4** and the data are summarized in Table 2.

The substituent groups on the C2 atom appear to have a significant impact on the energy of both the purple-blue peak and the green-yellow peak with the emission energy of **3** and **4** being the lowest. In all cases, the low energy emission peak is unaffected by the presence of oxygen and possesses decay

dx.doi.org/10.1021/om500757r | *Organometallics* XXXX, XXX, XXX–XXX

Table 1. Selected Bond Lengths (Å) and Angles (deg) of Compounds 1−4

compd	bond lengths		bond angles		φ [C(10)→B→N→C(1)]
1	B−N	1.428(2)	C(10)—B−N	120.24(15)	156.3(2)
	B−C(10)	1.592(2)	N−B—C(19)	119.63(14)	
	B−C(19)	1.582(4)	C(19) —B−C(10)	120.11(13)	
1[a]	B−N	1.440(1)	C(10)—B−N	121.4(1)	155.3(1)
	B−C(10)	1.600(1)	N−B—C(19)	119.5(1)	
	B−C(19)	1.595(1)	C(19) —B−C(10)	119.0(1)	
2[a]	B−N	1.442(1)	C(10)—B−N	119.4(1)	154.2(1)
	B−C(10)	1.601(1)	N−B—C(19)	121.9(1)	
	B−C(19)	1.596(1)	C(19) —B−C(10)	118.7(1)	
3[a]	B−N	1.440(1)	C(10)—B−N	119.4(1)	155.3(1)
	B−C(10)	1.601(1)	N−B—C(19)	122.1(1)	
	B−C(19)	1.596(1)	C(19) —B−C(10)	118.5(1)	
4[a]	B−N	1.442(1)	C(10)—B−N	119.4(1)	154.1(1)
	B−C(10)	1.601(1)	N−B—C(19)	122.2(1)	
	B−C(19)	1.597(1)	C(19) —B−C(10)	118.4(1)	

[a]Values obtained from DFT optimized geometries.

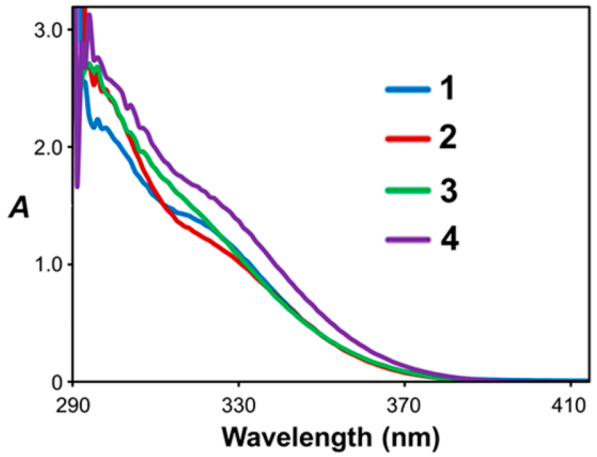

Figure 5. UV/vis spectra of **1**−**4** in THF at 10^{-4} M.

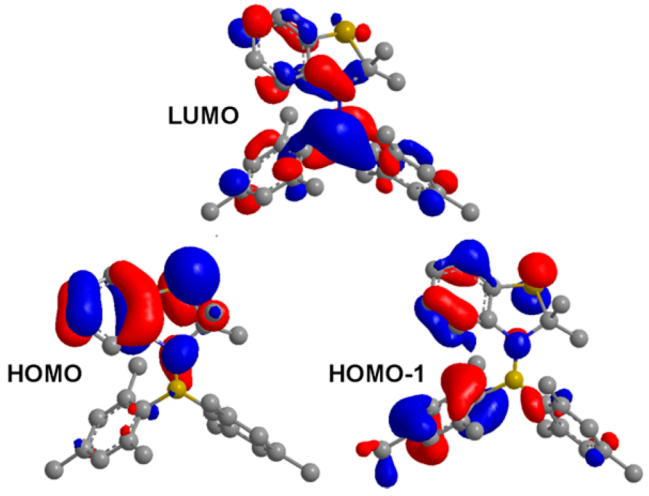

Figure 6. HOMO, HOMO−1, and LUMO diagrams of **1** (isocontour = 0.035).

lifetimes on the order of nanoseconds, indicating that phosphorescence is not responsible for this unusual phenomena. Furthermore, we observed no substantial change in the UV−vis absorption maxima with increasing concentration for all four compounds (see SI) which, in conjunction with the lack

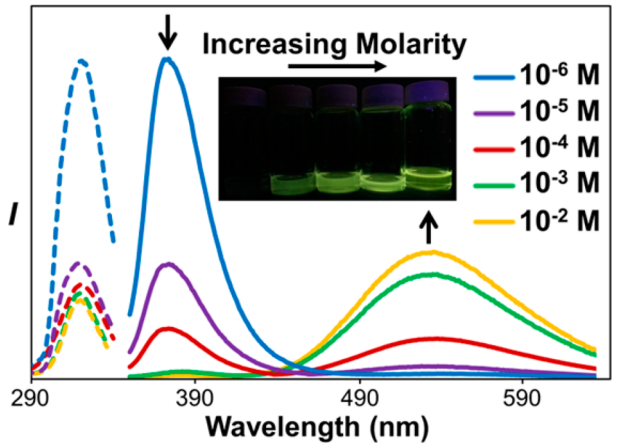

Figure 7. Fluorescence excitation (dotted) and emission (solid) spectra and photographs illustrating the concentration dependent emission (λ_{ex} = 318 nm) of **1** in THF.

of detectable nanoparticles by dynamic light scattering experiments (see SI), suggests that aggregation induced emission (AIE) is not responsible for this phenonmenon.[14] We therefore propose that the low energy emission band is a result of excimer fluorescence. To further probe the origin of the monomer and excimer emission from **1**−**4**, we examined the solvent dependence of the fluorescence. As shown in Figure 8 (and SI), a bathochromic shift was observed for both the monomer and excimer emission peaks of **1**−**4** with increasing solvent polarity, which is consistent with a polarized excited state involving charge transfer (CT) transitions for both emission peaks.

For the monomer emission, the solvent-dependent phenomenon agrees with the TD-DFT data that revealed the transition to the first excited state is dominated by a benzo-S to B (π^*) CT transition. For the excimer emission, we believe that it likely involves intermolecular charge transfer from the S atom (lone pair) to the benzo ring (π^*) via the dimer formation as revealed by the crystal structure shown in Figure 3. In fact, the lone pair of electrons on the sulfur atom are dominant in the HOMO and HOMO−1 orbitals of the molecules while the benzo π^* orbitals have significant contributions to both LUMO and LUMO+1 orbitals. Thus, energetically favorable inter-

dx.doi.org/10.1021/om500757r | Organometallics XXXX, XXX, XXX−XXX

Table 2. Pertinent Photophysical Data of 1−4 recorded in THF

compd	λ_{abs} (nm) (ε, L mol^{-1} cm^{-1})	λ_{em} monomer/excimer (nm)	τ monomer/excimer (ns ± 0.2)	Φ_{soln} excimer (%)
1	318 (1.23×10^4)	374/534	1.9/1.8	0.98
2	319 (1.17×10^4)	373/530	1.9/2.0	1.01
3	321 (1.16×10^4)	387/552	1.6/2.2	1.04
4	322 (1.51×10^4)	383/539	1.8/2.0	0.95

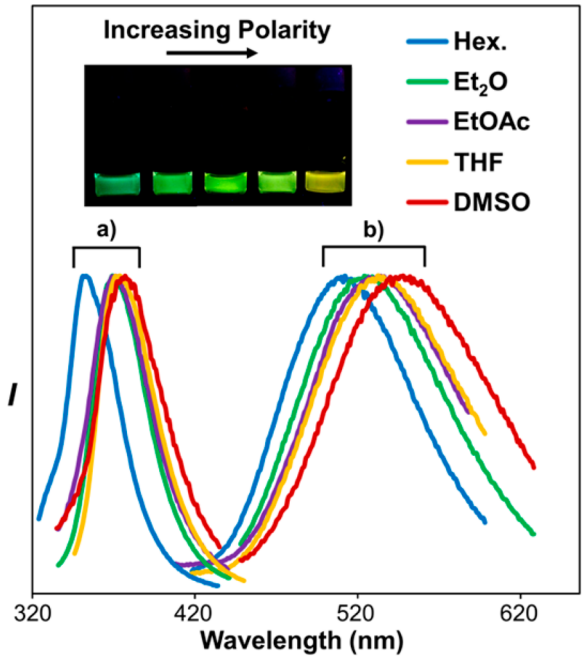

Figure 8. Fluorescence spectra of 1 at (a) 10^{-6} M and (b) 10^{-2} M in various solvents (λ_{ex} = 318 and 330 nm, respectively). Inset: photograph of each 10^{-2} M solution under a 365 nm UV lamp.

molecular interactions involving these two moieties in the excited state could be possible. This is further supported by the electrostatic potential (ESP) surfaces of each compound (see SI), which predict a buildup of negative and positive charge at the lone pairs on sulfur and the aromatic C−H's of the benzo ring. Additionally, the benzo ring appears to be less negatively charged in comparison to the two mesityl's, which would also contribute to the aforementioned intermolecular interaction. The involvement of the B atom in the excimer emission is also likely because it is conjugated with the benzo ring via the N atom and dominates the LUMO level. Similar short contact excimer fluorescence[15] has been observed for several derivatives of anthracene; however, there are only a limited number of these examples. More commonly observed is the π-stacking of flat aromatic molecules (pyrene) in the excited state,[16] which possess significantly longer decay lifetimes[16d] in comparison to their short contact counterparts.[15a,e] Given that our excimer lifetimes are relatively short, our short contact hypothesis remains feasible, although π-stacking interaction is also a possibility. There is a clear red shift in the monomer and excimer emission λ_{max} from the aliphatic (1 and 2) to the cyclic (3 and 4) substituted compounds, which may be attributed to the additional vibrational states due to the conformational change of the cyclopentyl and the cyclohexyl ring.

Further evidence that supports the assignment of the excimer emission in 1−4 is the distinct and unusual temperature dependence of the low energy emission peak.

In the temperature range of 80 °C to −78 °C, the low energy emission peak of 1 in 2-Me-THF experiences a bathochromic shift with decreasing temperature (Figure 9), changing emission

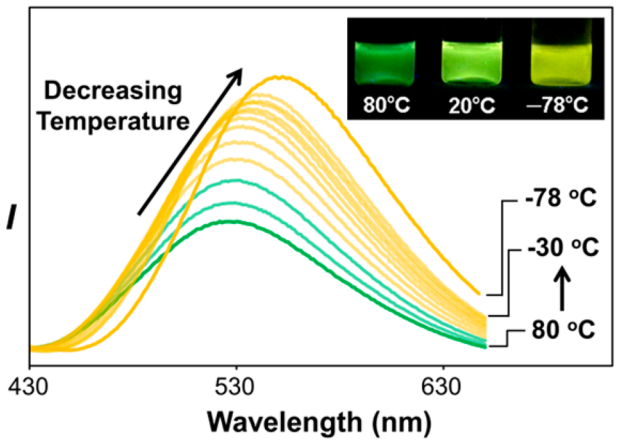

Figure 9. Fluorescence spectra of 1 in MeTHF (10^{-2} M) at various temperatures (10 °C intervals except for −78 °C). Inset: photograph of the solution at three select temperatures.

color from green to yellow while increasing emission intensity. This corresponds to a 0.15 nm/°C shift in λ_{max} (Figure 10),

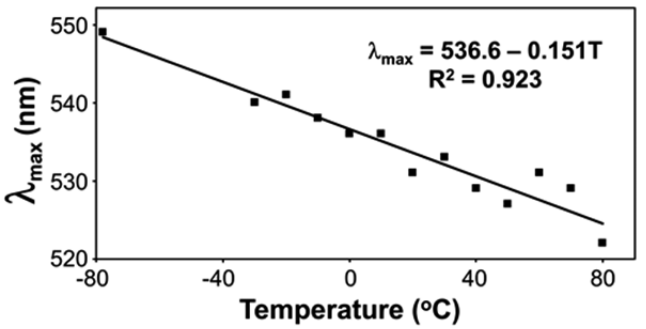

Figure 10. Temperature dependence of emission maxima for 1.

which is approximately half of that reported by Yang and co-workers for pyrene-functionalized organoboron compounds.[8] Similarly, 2−4 display red shifts of their low energy emission peaks with decreasing temperature of 0.10, 0.14, and 0.13 nm/°C respectively. In contrast, the monomer emission λ_{max} of 1−4 does not change within this temperature range, which could allow these compounds to be used for emission wavelength-based ratiometric temperature sensing (see SI). Due to instrument limitations, we were not able to monitor the spectral change for temperatures between −78 °C and −196 °C. At very low temperature (77 K, frozen 2-Me THF glass), the excimer peak of each compound vanishes completely and is replaced by an equally broad emission peak with λ_{max} = 479 nm (see SI). Similar emission bands were also observed in the solid

dx.doi.org/10.1021/om500757r | Organometallics XXXX, XXX, XXX−XXX

state fluorescence spectra of **1**−**4** (see SI) and have been assigned as emission from van der Waals dimers that are being directly photoexcited.[17] To better illustrate, the potential energy diagram of two monomer units at varying intermolecular distance and molecular orbital overlap is shown in Figure 11. At low monomer concentration (i.e., large intermolecular separation), the individual monomers are excited and emit photons prior to interacting with other monomer units. As the concentration is increased, van der Waals (vdW) dimers begin to form in equilibrium with the separate monomer units. Upon photoexcitaiton in solution, the excess internal energy of the system allows the vdW excited dimer to excimer activation barrier to be crossed, and a photon is released from the newly formed excited state dimer. Although similar excitations will occur in the solid state and at 77K, the lack of kinetic energy and rigid nature of the media do not allow the barrier to be crossed and a higher energy photon is emitted as a result of vdW dimer relaxtion.

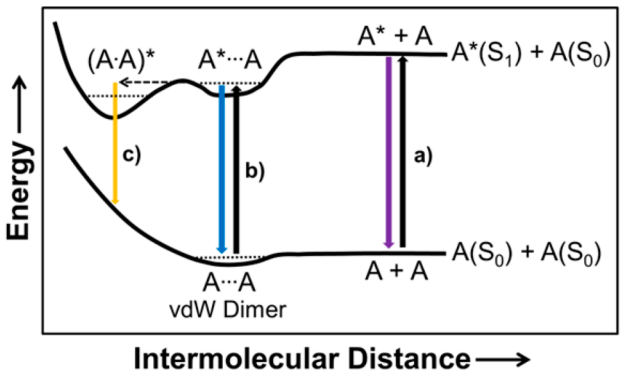

Figure 11. Potential energy diagram showing the origin of (a) monomer, (b) vdW dimer in the solid state and at 77K, and (c) excimer fluorescence, where each monomer unit is represented by A.

Given that the emission energy difference between the vdW dimer and excimer is small, it is conceivable that the geometric configuration of these two different emitting entities are alike which suggests our proposed mechanism of excimer formation may be correct. Although the fluorescence intensity and decay lifetimes[7] of organic compounds are expected to change with temperature, the red shift in emission maxima with decreasing temperature is unusual and has only been observed in a few organoboron-based systems.[8] For molecules **1**−**4**, the emission maxima red shift of the low energy peak could be explained by the increased molecular aggregation and greater intermolecular interactions with decreasing temperature. This temperature-dependent behavior of the low energy emission peak of **1**−**4** is consistent with typical excimer emission.[18]

The temperature dependence of the excimer emission of **1**−**4** was also found to persist in solvents of varying polarity such as hexanes and DMSO (see SI). Because of the polarized nature of the excimers formed by **1**−**4**, it is not surprising that the magnitude of the bathochromic shift in λ_{max} emission with decreasing temperature becomes smaller as the solvent polarity decreases. For example, the bathochromic shift of **1** in hexanes was found to be 0.03 nm/°C compared to a shift of 0.15 and 0.12 nm/°C in 2-Me-THF and DMSO respectively. The proposed excimer-based temperature dependent fluorescence of **1**−**4** is in rather stark contrast to the previously reported temperature-dependent fluorescence of triarylboron compounds, which were attributed to two competing intramolecular excited states (e.g., the locally excited vs twisted intramolecular charge transfer states reported by Yang et al.[8a] and the locally excited versus excited-state intramolecular proton transfer by Yamaguchi et al.[6e]). The electron-rich and nonconjugated thiazoline ring in these molecules are believed to be responsible for the excimer emission in compounds **1**−**4** because similar excimer emission phenomenon was not observed in related B═N-containing compounds that have a conjugated backbone such as indolyl.[10]

Compounds **1**−**4** represent a new class of temperature-dependent fluorescent molecules; however, they are not suitable for practical use as fluorescent thermometers because of their poor stability under ambient conditions and their low fluorescent quantum yields. In any case, these findings are a nice proof of concept as it is plausible that simple and robust luminescent thermometers may be achieved with further modification of the steric and electronic properties of this class of compounds.

CONCLUSIONS

In summary, we have synthesized and characterized a novel class of B═N-containing organoboron compounds. Despite the nonconjugated nature of the backbones, these molecules all display dual emission with a distinct green or yellow excimer fluorescent peak. Both the monomer and excimer fluorescence appear to be due to CT from sulfur to boron which is supported by TD-DFT and the positive solvatochromic behavior of each emission profile. Remarkably, the excimer fluorescence maxima were also found to be sensitive toward temperature, which could eventually lead to the design and use of new fluorescent and dual emissive compounds in molecular thermometry.

EXPERIMENTAL SECTION

General Procedures. All reactions were carried out under an inert atmosphere of dry nitrogen while employing standard Schlenk techniques. Aminothiophenol and all ketones were purchased from Aldrich chemical company, while $BMes_2F$ was purchased from TCI chemical company, and used without further purification. Solvents were taken from a PURE SOLV activated alumina column system (Innovative Technology Inc.), degassed using three freeze−pump−thaw cycles, and further dried over 4° molecular sieves for several days prior to use. ^{1}H, ^{13}C, and ^{11}B NMR spectra were recorded on a Bruker Avance 400 MHz spectrometer using deuterated solvents that were purchased from Cambridge Isotopes, degassed by vigorous dry nitrogen bubbling, and stored over 4° molecular sieves for several days prior to use. High-resolution mass spectra (HRMS) were obtained using a Micromass GCT TOF-EI Mass Spectrometer. Elemental analyses were performed by the Elemental Analysis Service at the University of Montreal. Excitation and emission spectra were recorded using a Photon Technologies International QuantaMaster Model 2 spectrometer equipped with a Quantum Northwest TLC 50 Temperature-Controlled Cuvette Holder. Luminescent decay lifetimes were measured against an instrument response function (IRF) and fitted using a single exponential fitting curve (determined and fitted curves can be found in the SI). UV−visible spectra were recorded a Varian Cary 50 spectrometer. Photoluminescent quantum yields were measured using the optically dilute method ($A \approx 0.1$) at room temperature in dry/degassed

dx.doi.org/10.1021/om500757r | Organometallics XXXX, XXX, XXX−XXX

THF relative to quinine sulfate in 0.5 M H_2SO_4 (Φ_{sol} = 0.546).[19]

Ligand Synthesis. All benzothiazoline ligands were prepared, purified, and characterized in accordance with procedures described in the literature.[9]

2,2-Dimethylbenzothiazoline. The title compound was obtained as a pale yellow solid in 80% yield. ^{1}H NMR (400 MHz, $CDCl_3$): δ 7.09 (d, J = 7.6 Hz, 1H, Ar−H), 6.94 (t, J = 7.7 Hz, 1H, Ar−H), 6.79 (t, J = 7.4 Hz, 1H, Ar−H), 6.69 (d, J = 7.8 Hz, 1H, Ar−H), 3.99 (br s, 1H, N−H), 1.76 (s, 6H, $-CH_3 \times 2$) ppm.

(±) 2,2-Ethylmethylbenzothiazoline. The title compound was obtained as a yellow oil in 71% yield. ^{1}H NMR (400 MHz, $CDCl_3$): δ 7.07 (d, J = 7.6 Hz, 1H, Ar−H), 6.93 (t, J = 7.6 Hz, 1H, Ar−H), 6.76 (t, J = 7.6 Hz, 1H, Ar−H), 6.66 (d, J = 7.8 Hz, 1H, Ar−H), 3.96 (br s, 1H, N−H), 1.95 (m, 2H, $-CH_2$), 1.70 (s, 3H, $-CH_3$), 1.08 (t, J = 7.30, 3H, $-CH_2-\mathbf{CH_3}$) ppm.

Spiro[benzothiazoline-2,1′-cyclopentane]. The title compound was obtained as a yellow oil in 74% yield. ^{1}H NMR (400 MHz, $CDCl_3$): δ 7.08 (d, J = 7.6 Hz, 1H, Ar−H), 6.93 (t, J = 7.6 Hz, 1H, Ar−H), 6.78 (t, J = 7.6 Hz, 1H, Ar−H), 6.67 (d, J = 7.8 Hz, 1H, Ar−H), 4.09 (br s, 1H, N−H), 2.14 (m, 4H, cyclopentyl), 1.82 (quint, J = 3.53 Hz, 4H, cyclopentyl) ppm.

Spiro[benzothiazoline-2,1′-cyclohexane]. The title compound was obtained as a white solid in 69% yield. ^{1}H NMR (400 MHz, $CDCl_3$): δ 7.06 (d, J = 7.6 Hz, 1H, Ar−H), 6.92 (t, J = 7.7 Hz, 1H, Ar−H), 6.75 (t, J = 7.6 Hz, 1H, Ar−H), 6.66 (d, J = 7.7 Hz, 1H, Ar−H), 4.05 (br s, 1H, N−H), 2.28−2.19 (overlapping s, 2H, cyclohexyl), 1.85−1.54 (m, 7H, cyclohexyl), 1.32 (m, 1H, cyclohexyl) ppm.

General Procedure for the Syntheses of the Boron Compounds 1−4. A 125 mL oven-dried Schlenk flask was charged with sodium hydride (72 mg, 3.1 mmol), benzothiazoline derivative (∼500 mg, 3.1 mmol), THF (30 mL), and a magnetic stir bar. The mixture was then stirred at room temperature for 1 h with white precipitate observed after 15 min. $BMes_2F$ (∼800 mg, 3.1 mmol) in THF (5 mL) was then added dropwise at room temperature, resulting in a clear pale yellow solution which fluoresced green/yellow upon 365 nm irradiation. The mixture was allowed to stir overnight, before being diluted with petroleum ether and concentrated in vacuo. Flash column chromatography with 3:2 hexane/CH_2Cl_2 (**1**) or petroleum ether (**2**−**4**) as the eluent afforded the desired products in moderate yields (50−58%). The compounds were further purified by either recrystallization from the slow evaporation of CH_2Cl_2 (**1**) or precipitation from petroleum ether at −25 °C (**2**−**4**).

*B(Mesityl)$_2$(N-2,2-dimethylbenzothiazoline) (**1**).* The title compound was obtained as a white grain-like solid, 50% yield. ^{1}H NMR (400 MHz, CD_2Cl_2): δ 7.06 (d, J = 8.0 Hz, 1H, Ar−H), 6.79 (t, J = 7.3 Hz, 1H, Ar−H), 6.70 (s, 2H, Mes), 6.52 (s, 2H, Mes), 6.44 (t, J = 7.3 Hz, 1H, Ar−H), 6.50 (d, J = 8.1 Hz, 1H, Ar−H), 2.17 (s, 9H, Mes $-CH_3 \times 3$), 2.08 (s, 3H, Mes $-CH_3$), 1.97 (s, 6H, Mes $-CH_3 \times 2$), 1.52 (s, 6H, benzothiazoyl $-CH_3 \times 2$) ppm; ^{13}C NMR (100 MHz, CD_2Cl_2) δ 146.0 (Ar), 141.7 (Mes), 140.2 (Mes), 138.1 (Mes), 137.8 (Mes), 133.0 (Ar), 128.6 (Mes), 128.4 (Mes), 124.7 (Ar), 123.9 (Ar), 122.6 (Ar), 121.2 (Ar), 81.8 (benzothiazoyl C2), 29.6 (Me × 2), 23.6 (Mes), 22.2 (Mes), 21.2 (Mes), 21.1 (Mes) ppm; ^{11}B NMR (128 MHz, CD_2Cl_2) δ 47.8 ppm; HRMS (EI) calcd for $C_{27}H_{32}BNS$ $[M]^+$, 413.2354; found, 413.2348. Anal. Calcd for $C_{27}H_{32}BNS$: C, 78.44; H, 7.80; N, 3.39; S, 7.76. Found: C, 78.34; H, 7.90; N, 3.32; S, 7.87.

*B(Mesityl)$_2$(N-(±)-2,2-ethylmethylbenzothiazoline) (**2**).* The title compound was obtained as a white flaky solid, 55% yield. ^{1}H NMR (400 MHz, CD_2Cl_2): δ 7.03 (d, J = 7.5 Hz, 1H, Ar−H), 6.76 (t, J = 7.5 Hz, 1H, Ar−H), 6.72 (s, 1H, Mes), 6.65 (s, 1H, Mes), 6.54 (s, 1H, Mes), 6.49 (s, 1H, Mes), 6.47 (t, J = 7.6 Hz, 1H, Ar−H), 6.42 (d, J = 7.7 Hz, 1H, Ar−H), 2.27 (br s, 3H, Mes), 2.16 (s, 3H, Mes), 2.08 (s, 3H, Mes), 2.06 (s, 3H, Mes), 2.01 (s, 3H, Mes), 1.95 (s, 3H, Mes), 1.72 (m, 2H, $-CH_2-CH_3$), 1.43 (s, 3H, benzothiazoyl $-CH_3$), 0.81 (t, J = 7.2 Hz, 1H, $-CH_2-CH_3$) ppm; ^{13}C NMR (100 MHz, CD_2Cl_2) δ 147.0 (Ar), 142.0 (Mes), 141.5 (Mes), 140.3 (Mes), 140.0 (Mes), 138.0 (Mes), 137.8 (Mes), 132.7 (Ar), 128.7 (Mes), 128.6 (Mes), 128.3 (Mes), 124.5 (Ar), 123.8 (Ar), 122.3 (Ar), 120.9 (Ar), 87.0 (benzothiazoyl C2), 35.4 (benzothiaozyl C2 Ethyl), 26.6 (benzothiazoyl C2Methyl), 24.2 (Mes), 23.1 (Mes), 22.6 (Mes), 21.9 (Mes), 21.2 (Mes), 21.1 (Mes), 11.1 (benzothiazoyl C2 Ethyl) ppm; ^{11}B NMR (128 MHz, CD_2Cl_2) δ 48.1 ppm; HRMS (EI) calcd for $C_{28}H_{34}BNS$ $[M]^+$, 427.2510; found, 427.2523. Anal. Calcd for $C_{28}H_{34}BNS$: C, 78.68; H, 8.02; N, 3.28; S, 7.50. Found: C, 78.72; H, 8.14; N, 3.27; S, 7.55.

*B(Mesityl)$_2$(N-Spiro[benzothiazoline-2,1′-cyclopentane]) (**3**).* The title compound was obtained as a white flaky solid, 45% yield. ^{1}H NMR (400 MHz, CD_2Cl_2): δ 7.21 (d, J = 7.7 Hz, 1H, Ar−H), 6.93(t, J = 7.4 Hz, 1H, Ar−H), 6.81 (s, 2H, Mes), 6.64 (s, 2H, Mes), 6.62 (t, J = 7.5 Hz, 1H, Ar−H), 6.60 (d, J = 7.6 Hz, 1H, Ar−H), 2.31 (br s, 9H, Mes $-CH_3 \times 3$), 2.21 (s, 3H, Mes $-CH_3$), 2.19−2.11 (m, 4H, cyclopenthyl), 2.09 (s, 6H, Mes $-CH_3 \times 2$), 1.77−1.54 (m, 4H, cyclopentyl) ppm; ^{13}C NMR (100 MHz, CD_2Cl_2) δ 147.1 (Ar), 141.8 (Mes), 140.1 (Mes), 138.0 (Mes), 137.7 (Mes), 133.2 (Ar), 128.6 (Mes), 128.4 (Mes), 124.6 (Ar), 123.8 (Ar), 122.9 (Ar), 120.8 (Ar), 93.4 (benzothiazoyl C2), 37.5 (cyclopentyl), 23.6 (cyclopentyl), 22.4 (Mes), 22.2 (Mes), 21.2 (Mes), 21.1 (Mes) ppm; ^{11}B NMR (128 MHz, CD_2Cl_2) δ 48.3 ppm; HRMS (EI) calcd for $C_{29}H_{34}BNS$ $[M]^+$, 439.2510; found, 439.2515. Anal. Calcd for $C_{29}H_{34}BNS$: C, 79.26; H, 7.80; N, 3.19; S, 7.30. Found: C, 79.29; H, 7.90; N, 3.03; S, 7.39.

*B(Mesityl)$_2$(N-Spiro[benzothiazoline-2,1′-cyclohexane]) (**4**).* The title compound was obtained as a pale yellow flaky solid, 58% yield. ^{1}H NMR (400 MHz, CD_2Cl_2): δ 7.19 (d, J = 7.5 Hz, 1H, Ar−H), 6.89 (t, J = 7.6 Hz, 1H, Ar−H), 6.82 (s, 2H, Mes), 6.64 (s, 2H, Mes), 6.62 (t, J = 7.5 Hz, 1H, Ar−H), 6.59 (d, J = 7.8 Hz, 1H, Ar−H), 2.31 (br s, 9H, Mes $-CH_3 \times 3$), 2.21 (s, 3H, Mes $-CH_3$), 2.11 (s, 6H, Mes $-CH_3 \times 2$), 1.92−1.82 (m, 2H, cyclohexyl), 1.65−1.56 (m, 6H, cyclohexyl), 0.97−0.84 (m, 3H, cyclohexyl) ppm; ^{13}C NMR (100 MHz, CD_2Cl_2) δ 146.9 (Ar), 141.8 (Mes), 140.0 (Mes), 137.9 (Mes), 137.7 (Mes), 132.9 (Ar), 128.6 (Mes), 128.4 (Mes), 124.4 (Ar), 123.7 (Ar), 122.5 (Ar), 121.5 (Ar), 90.2 (benzothiazoyl C2), 37.4 (cyclohexyl), 25.5 (cyclohexyl), 23.7 (Mes), 22.3 (Mes), 21.2 (Mes), 21.1 (Mes) ppm; ^{11}B NMR (128 MHz, CD_2Cl_2) δ 48.3 ppm; HRMS (EI) calcd for $C_{30}H_{36}BNS$ $[M]^+$, 453.2667; found, 453.2659. Anal. Calcd for $C_{30}H_{36}BNS$: C, 79.46; H, 8.00; N, 3.09; S, 7.07. Found: C, 79.53; H, 8.17; N, 3.09; S, 7.13.

Computational Modeling. All calculations were performed using the Gaussian 09 suite of programs[20] on the High Performance Computing Virtual Laboratory (HPCVL) at Queen's University. Initial input coordinates for **1** were taken from its crystal structure data while **2**− **4** were generated using

dx.doi.org/10.1021/om500757r | Organometallics XXXX, XXX, XXX−XXX

the optimized geometry of **1** as the starting point. Ground state geometry optimizations and TD-DFT vertical excitations were computed using the B3LYP[21] level of theory and 6-311+(d,p)[22] Pople-style basis set for all atoms. Bulk solvent effects were accounted for implicitly in all calculations through the use of the integral equation formulation polarizable continuum model (IEF-PCM) with tetrahydrofuran (THF) as the solvent.[23]

Dynamic Light Scattering. Measurements were performed at a scattering angle of 90° at 20 °C using a Brookhaven 9025 instrument equipped with a He−Ne laser operating at 632.8 nm. Samples were prepared by dissolving the desired compounds in 2-Me-THF, which had been passed through a 0.1 μm filter several times, to give solutions of concentration $\sim 10^{-3}$ M. The data were analyzed by the cumulant method[24] to give the average size of particles in solution.

X-ray Crystal Structure Determination of 1. Colorless block crystals suitable for single-crystal X-ray diffraction were grown by slow evaporation of a concentrated dichloromethane solution of **1**. The crystal ($0.20 \times 0.10 \times 0.10$ mm^3) was mounted on a glass fiber, and diffraction data were collected on a Bruker Apex II single-crystal X-ray diffractometer with graphite-monochromated Mo Kα radiation, operating at 50 kV and 30 mA (T = 180 K). Data were processed using the Bruker SHELXTL software package (version 6.10)[25] and corrected for absorption effects. The crystal of **1** belongs to the monoclinic space group $P2_1/n$. All non-hydrogen atoms were refined anisotropically. The crystal data of **1** have been deposited at the Cambridge Crystallographic Data Center (CCDC No. 1015484). Complete crystal structure data can be found in the SI.

■ ASSOCIATED CONTENT

Ⓢ Supporting Information

CIF files, figures and tables giving NMR spectra of all compounds, crystal structure data for **1**, TD-DFT calculation data, and all additional UV−vis/fluorescence data of **1**−**4**. This material is available free of charge via the Internet at http://pubs.acs.org.

■ AUTHOR INFORMATION

Corresponding Author

*E-mail: wangs@chem.queensu.ca.

Notes

The authors declare no competing financial interest.

■ ACKNOWLEDGMENTS

We thank the Natural Sciences and Engineering Research Council for financial support, the High Performance Computing Virtual Laboratory at Queen's for computational facilities, and Jian Wang for performing the DLS measurements.

■ REFERENCES

(1) (a) Yuan, Z.; Taylor, N. J.; Marder, T. B.; Williams, I. D.; Kurtz, S. K.; Cheng, L. T. *Chem. Commun.* **1990**, 1489−1492. (b) Yuan, Z.; Taylor, N. J.; Ramanchandran, R.; Marder, T. B. *Appl. Organomet. Chem.* **1996**, *10*, 305−316. (c) Yamaguchi, S.; Shirasaka, T.; Tamao, K. *Org. Lett.* **2000**, *2*, 4129−4132. (d) Lambert, C.; Stadler, S.; Bourhill, G.; Brauchle, C. *Angew. Chem., Int. Ed.* **1996**, *35*, 644−646. (e) Wu, Q.; Esteghamation, M.; Hu, N. X.; Popovic, Z.; Enwright, G.; Tao, Y.; D'Iorio, M.; Wang, S. *Chem. Mater.* **2000**, *12*, 79−83. (f) Esteghamation, M.; Hu, N. X.; Popvic, Z.; Enwright, G.; Breeze, S. R.; Wang, S. *Angew. Chem., Int. Ed.* **1999**, *38*, 985−988. (g) Wade, C. R.; Broomsgrove, A. E. J.; Aldridge, S.; Gabbaï, F. P. *Chem. Rev.* **2010**, *110*, 3958−3984. (h) Jäkle, F. *Chem. Rev.* **2010**, *110*, 3985−4022. (i) Chen, P.; Lalancette, R. A.; Jäkle, F. *Angew. Chem., Int. Ed.* **2012**, *51*, 7994−7998.

(2) (a) Matsumi, N.; Naka, K.; Chujo, Y. *J. Am. Chem. Soc.* **1998**, *30*, 833−837. (b) Noda, T.; Ogawa, H.; Shirota, Y. *Adv. Mater.* **1999**, *11*, 283−285. (c) Kido, J.; Kimura, M.; Nagai, K. *Chem. Lett.* **2001**, 47. (d) Branger, C.; Lequan, M.; Lequan, R. M.; Barzoukas, M.; Fort, A. *J. Mater. Chem.* **1996**, *6*, 555−558. (e) Corriu, R. J. P.; Deforth, T.; Douglas, W. E.; Guerrero, G.; Siebert, W. S. *Chem. Commun.* **1998**, 963−964. (f) Kaim, W.; Schulz, A. *Angew. Chem., Int. Ed.* **1984**, *23*, 615−616. (g) Albrecht, K.; Kaiser, V.; Boese, R.; Adams, J.; Kaufmann, D. E. *J. Chem. Soc., Perkin Trans. 2* **2000**, 2153−2157. (h) Jia, W. L.; Moran, M. J.; Yuan, Y. Y.; Lu, Z. H.; Wang, S. N. *J. Mater. Chem.* **2005**, *15*, 3326−3333.

(3) (a) Nagura, K.; Saito, S.; Frohlich, R.; Glorius, F.; Yamaguchi, S. *Angew. Chem., Int. Ed.* **2012**, *51*, 7762−7766. (b) Rao, Y. .; Amarne, H.; Zhao, S. B.; McCormick, T. M.; Martic, S.; Sun, Y.; Wang, R. Y.; Wang, S. *J. Am. Chem. Soc.* **2008**, *130*, 12898−12900. (c) Baik, C.; Hudson, Z. M.; Amarne, H.; Wang, S. *J. Am. Chem. Soc.* **2009**, *131*, 14549−14559. (d) Amarne, H.; Baik, C.; Murphy, S. K.; Wang, S. *Chem.—Eur. J.* **2010**, *16*, 4750−4761. (e) Rao, Y. L.; Chen, L. D.; Mosey, N. J.; Wang, S. *J. Am. Chem. Soc.* **2012**, *134*, 11026−11034. (f) Lu, J. S.; Ko, S. B.; Walters, N. R.; Kang, Y.; Sauriol, F.; Wang, S. *Angew. Chem., Int. Ed.* **2013**, *52*, 4544−4548. (g) Rao, Y. L.; Amarne, H.; Lu, J. S.; Wang, S. *Dalton Trans.* **2013**, *42*, 638−644. (h) Rao, Y. L.; Amarne, H.; Chen, L. D.; Brown, M. L.; Mosey, N. J.; Wang, S. *J. Am. Chem. Soc.* **2013**, *135*, 3407−3410. (i) Rao, Y. L.; Horl, C.; Braunschweig, H.; Wang, S. *Angew. Chem., Int. Ed.* **2014**, *53*, 9086−9089.

(4) (a) Shuto, A.; Kushida, T.; Fukushima, T.; Kaji, H.; Yamaguchi, S. *Org. Lett.* **2013**, *15*, 6234−6237. (b) Li, D.; Zhang, H.; Wang, Y. *Chem. Soc. Rev.* **2013**, *42*, 8416−8433. (c) Hellstrom, S. L.; Ugolotti, J.; Britovsek, G. J. P.; Jones, T. S.; White, A. J. P. *New J. Chem.* **2008**, *32*, 1379−1387. (d) Qin, Y.; Kiburu, I.; Shah, S.; Jakle, F. *Org. Lett.* **2006**, *8*, 5227−5230. (e) Qin, Y.; Pagba, C.; Piotrowiak, P.; Jakle, F. *J. Am. Chem. Soc.* **2004**, *126*, 7015−7018. (f) Zhang, Z.; Huo, C.; Zhang, J.; Zhang, P.; Tian, W.; Wang, Y. *Chem. Commun.* **2006**, 281−283.

(5) (a) Zhou, Z.; Xiao, S. Z.; Xu, J.; Liu, Z. Q.; Shi, M.; Luang, C. H. *Org. Lett.* **2006**, *8*, 3911−3914. (b) Lemieux, V.; Spantulescu, M. D.; Bladridge, K. K.; Branda, N. R. *Angew. Chem., Int. Ed.* **2008**, *47*, 5034−5037. (c) Kano, N.; Yoshino, J.; Kawashima, T. *Org. Lett.* **2005**, *7*, 3909−3911.

(6) For recent examples of dual emissive organoboron compounds that are caused by intramolecular electronic transitions, see: (a) Samonina-Kosicka, J.; DeRosa, C. A.; Morris, W. A.; Fan, Z.; Fraser, C. L. *Macromolecules* **2014**, *47*, 3736−3746. (b) Swamy P, C. A.; Mukherjee, S.; Thilagar, P. *Inorg. Chem.* **2014**, *53*, 4813−4823. (c) Sun, X.; Zhang, X.; Li, X.; Liu, X.; Zhang, G. *J. Mater. Chem.* **2012**, *22*, 17332−17339. (d) Xu, S.; Evans, R. E.; Liu, T.; Zhang, G.; Demas, J. N.; Trindle, C. O.; Fraser, C. L. *Inorg. Chem.* **2013**, *52*, 3597−3610. (e) Suzuki, N.; Fukazawa, A.; Nagura, K.; Saito, S.; Kitoh-Nishioka, H.; Yokogawa, D.; Irle, S.; Yamaguchi, S. *Angew. Chem., Int. Ed.* **2014**, *53*, 8231−8235. (f) Wong, H. L.; Wong, W. T.; Yam, V. W. W. *Org. Lett.* **2012**, *14*, 1862−1865. (g) Li, Y.; Kang, Y.; Lu, J. S.; Wyman, I.; Ko, S. B.; Wang, S. *Organometallics* **2014**, *33*, 964−973.

(7) (a) Gota, C.; Okabe, K.; Funatsu, T.; Harada, Y.; Uchiyama, S. *J. Am. Chem. Soc.* **2009**, *131*, 2766−2767. (b) Yang, J. M.; Yang, H.; Lin, L. *ACS Nano* **2011**, *5*, 5067−5071. (c) Brites, C. D.; Lima, P. P.; Silva, N. J.; Millan, A.; Amaral, V. S.; Palacio, F.; Carlos, L. D. *Nanoscales* **2012**, *4*, 4799−4829. (d) Ozawa, T.; Yoshimura, H.; Kim, S. B. *Anal. Chem.* **2013**, *85*, 590−609. (e) Takei, Y.; Arai, S.; Murata, A.; Takabayashi, M.; Oyama, K.; Ishiwata, S.; Takeoka, S.; Suzuki, M. *ACS Nano* **2014**, *8*, 198−206.

(8) (a) Feng, J.; Tian, K.; Hu, D.; Wang, S.; Li, S.; Zeng, Y.; Li, Y.; Yang, G. *Angew. Chem., Int. Ed.* **2011**, *50*, 8072−8076. (b) Feng, J.; Xiong, L.; Wang, S.; Li, S.; Li, Y.; Yang, G. *Adv. Funct. Mater.* **2013**, *23*, 340−345. (c) Pais, V. F.; Lassaletta, J. M.; Fernandez, R.; El-

Sheshtawy, H. S.; Ros, A.; Pichel, U. *Chem.—Eur. J.* **2014**, *20*, 7638−7645.
(9) Kodomari, M.; Satoh, A.; Nakano, R.; Aoyama, T. *Synth. Commun.* **2007**, *37*, 3329−3335.
(10) Cui, Y.; Li, F.; Lu, Z. H.; Wang, S. *Dalton Trans.* **2007**, 2634−2643.
(11) (a) Pestana, D. C.; Power, P. P. *Inorg. Chem.* **1991**, *30*, 528−535. (b) Lichtblau, A.; Hausen, H. D.; Schwarz, W.; Kaim, W. *Inorg. Chem.* **1993**, *32*, 73−78. (c) Lichtblau, A.; Kaim, W.; Schulz, A.; Strahl, T. *J. Chem. Soc., Perkin Trans.* **1992**, 1497−1500.
(12) Wiliams, D. H.; Fleming, I. *Spectroscopic Methods in Organic Chemistry*, 4th ed.; McGraw-Hill: London, 1987.
(13) (a) Rohr, A. D.; Kampf, J. W.; Ashe, A. J., III *Organometallics* **2013**, *33*, 1318−1321. (b) Braunschweig, H.; Geetharani, K.; Jimenez-Halla, J. O. C.; Schäfer, M. *Angew. Chem., Int. Ed.* **2014**, *53*, 3500−3504. (c) Xu, S.; Zakharov, L. N.; Liu, S.-Y. *J. Am. Chem. Soc.* **2011**, *133*, 20152−20155. (d) Abbey, E. R.; Zakharov, L. N.; Liu, S. Y. *J. Am. Chem. Soc.* **2008**, *130*, 7250−7252.
(14) (a) Chen, J.; Xu, B.; Ouyang, X.; Tang, B. Z.; Cao, Y. *J. Phys. Chem. A* **2004**, *108*, 7522−7526. (b) Luo, J.; Xie, Z.; Lam, J. W. Y.; Cheng, L.; Chen, H.; Qui, C.; Kwok, H. S.; Zhan, X.; Liu, Y.; Zhu, D.; Tang, B. Z. *Chem. Commun.* **2001**, 1740−1741. (c) Hong, Y.; Lam, J. W. Y.; Tang, B. Z. *Chem. Soc. Rev.* **2011**, *40*, 5361−5388. (d) Chen, J.; Law, C. C. W.; Lam, J. W. Y.; Dong, Y.; Lo, S. M. F.; Williams, I. D.; Zhu, D.; Tang, B. Z. *Chem. Mater.* **2003**, *15*, 1535−1546. (e) Hong, Y.; Lam, J. W. Y.; Tang, B. Z. *Chem. Commun.* **2009**, 4332−4353.
(15) (a) Zhang, G.; Yang, G.; Wang, S.; Chen, Q.; Ma, J. S. *Chem.—Eur. J.* **2007**, *13*, 3630−3635. (b) Hinoue, T.; Shigenoi, Y.; Sugino, M.; Mizobe, Y.; Hisaki, I.; Miyata, M.; Tohnai, N. *Chem.—Eur. J.* **2012**, *18*, 4634−4643. (c) Abe, Y.; Karasawa, S.; Koga, N. *Chem.—Eur. J.* **2012**, *18*, 15038−15048. (d) Lekha, P. K.; Prasad, E. *Chem.—Eur. J.* **2010**, *16*, 3699−3706. (e) Wang, L.; Wong, W. Y.; Lin, M. F.; Wong, W. K.; Cheah, K. W.; Tam, H. L.; Chen, C. H. *J. Mater. Chem.* **2008**, *18*, 4529−4536.
(16) (a) Birks, J. B.; Christophorou, L. G. *Spectrochim. Acta* **1963**, *19*, 401−410. (b) Dyson, D. J.; Munro, I. H.; Birks, J. B. *Proc. R. Soc. London, Ser. A* **1963**, *275*, 575−588. (c) Bains, G. K.; Kim, S. H.; Sorin, E. J.; Narayanaswami, V. *Biochemistry* **2012**, *51*, 6207−6219. (d) Kaanumalle, L. S.; Gibb, C. L. D.; Gibb, B. C.; Ramamurthy, V. *J. Am. Chem. Soc.* **2005**, *127*, 3674−3675 and references therein..
(17) (a) Saigusa, H.; Lim, H. C. *Acc. Chem. Res.* **1996**, *29*, 171−178. (b) Yip, W. T.; Levy, D. H. *J. Phys. Chem.* **1996**, *100*, 11539−11545.
(18) Chandrasekharan, N.; Kelly, L. *Spectrum* **2002**, *15*, 1−7.
(19) Brouwer, A. M. *Pure Appl. Chem.* **2011**, *83*, 2213−2228.
(20) Frisch, M. J.; Trucks, G. W.; Schlegel, H. B.; Scuseria, G. E.; Robb, M. A.; Cheeseman, J. R.; Scalmani, G.; Barone, V.; Mennucci, B.; Petersson, G. A. H.; Nakatsuji, M.; Caricato, X.; Li, H. P. F.; Hratchian, A.; Izmaylov, J.; Bloino, G.; Zheng, J. L.; Sonnenberg, M.; Hada, M.; Ehara, K.; Toyota, R.; Fukuda, J.; Hasegawa, M.; Ishida, T.; Nakajima, Y.; Honda, O.; Kitao, H.; Nakai, T.; Vreven, J. A.; Montgomery Jr., J. E.; Peralta, F.; Ogliaro, M.; Bearpark, J. J.; Heyd, E.; Brothers, K. N.; Kudin, V. N.; Staroverov, T.; Keith, R.; Kobayashi, J.; Normand, K.; Raghavachari, A.; Rendell, J. C.; Burant, S. S.; Iyengar, J.; Tomasi, M.; Cossi, N.; Rega, J. M.; Millam, M.; Klene, J. E.; Knox, J. B.; Cross, V.; Bakken, C.; Adamo, J.; Jaramillo, R.; Gomperts, R. E.; Stratmann, O.; Yazyev, A. J.; Austin, R.; Cammi, C.; Pomelli, J. W.; Ochterski, R. L.; Martin, K.; Morokuma, V. G.; Zakrzewski, G. A.; Voth, P.; Salvador, J. J.; Dannenberg, S.; Dapprich, A. D.; Daniels, O.; Farkas, J. B.; Foresman, J. V.; Ortiz, J.; Cioslowski, J.; Fox, D. J. *Gaussian 09*, revision C.01; Gaussian, Inc.: Wallingford, CT, 2010.
(21) (a) Becke, A. D. *Phys. Rev. A* **1988**, *38*, 3098−3100. (b) Becke, A. D. *J. Chem. Phys.* **1993**, *98*, 1372−1377. (c) Lee, C.; Yang, W.; Par, R. G. *Phys. Rev. B* **1988**, *37*, 785−789.
(22) (a) Ditchfield, R.; Hehre, W. J.; Pople, J. A. *J. Chem. Phys.* **1971**, *54*, 724−728. (b) McLean, A. D.; Chandler, G. S. *J. Chem. Phys.* **1980**, *72*, 5639−5648.
(23) Cancés, E.; Mennucci, B.; Tomasi, J. *J. Chem. Phys.* **1997**, *107*, 3032−3041.
(24) Berne, B. J. P.; Pecora, R. *Dynamic Light Scattering with Applications to Chemistry, Biology and Physics*;. Dover Pulications, Inc.: Mineola, NY, 2000.
(25) *SHELXTL*, version 6.14; Bruker AXS: Madison, WI, 2000−2003.